



# Development of a novel daily-scale compound dry and hot index and its application across non-arid regions of China

Huimin Wang<sup>1</sup>, Gengxi Zhang<sup>2</sup>, Shuyu Zhang<sup>3</sup>, Xiaoling Su<sup>1</sup>, Songbai Song<sup>1</sup>, Lijie Shi<sup>2</sup>, Kai Feng<sup>4</sup>, Xiaolei Fu<sup>2</sup>

- 5 <sup>1</sup> College of Water Resources and Architectural Engineering, Northwest A & F University, Yangling 712100, China  
<sup>2</sup> College of Hydraulic Science and Engineering, Yangzhou University, Yangzhou 225012, China  
<sup>3</sup> School of Environmental Science and Engineering, Southern University of Science and Technology, Shenzhen 518055, China  
<sup>4</sup> College of Water Conservancy, North China University of Water Resources and Electric Power, Zhengzhou 450046, China
- 10 *Correspondence to:* Gengxi Zhang (gengxizhang@yzu.edu.cn); Xiaoling Su (xiaolingsu@nwafu.edu.cn); and Xiaolei Fu (fuxiaolei518@yzu.edu.cn)

**Abstract.** Drought and heat extremes often occur simultaneously or sequentially within a short period, named compound dry and hot events (CDHEs), enhancing damages caused by individual drought or heat extremes. Under global warming, occurrences of short-term CDHEs have increased, adversely impacting the ecosystem and society. However, current indicators generally monitor CDHEs at monthly scales, which cannot reflect short-term CDHEs. This study proposes a novel daily-scale compound dry and hot index (DCDHI) by jointing daily Standardized Moisture Anomaly Index (SZI) and Standardized Temperature Index (STI) using Copula. The applicability of daily SZI and DCDHI indices in monitoring droughts and CDHEs is verified across non-arid regions of China. The daily SZI agrees better with soil moisture variations than the Standardized Precipitation Index (SPI) and Standardized Precipitation and Temperature Index (SPEI) at multiple time scales, indicating it can be applied to construct daily DCDHI for detecting compound dry and hot events. The DCDHI can detect spatial evolutions of dry and hot conditions within a month and reflects vegetation losses, indicating the DCDHI is a good indicator for detecting compound CDHEs at different time scales (daily to monthly). The characteristics of CDHEs during growing seasons (April to October) are also investigated from 1961 to 2021. There is a significant increase in the area affected by CDHEs, which occur more frequently for the period of 1990-2021 than 1961-1989. The severity of compound dry and hot events decreases from the period 1961-1989 to 1990-2021 in northern regions but increases in southern especially southwestern regions. More extreme compound dry and hot events are more likely to occur under global warming. The new tool proposed in this study could detect evolutions and characteristics of short-term CDHEs and provide technical support for the risk management of extreme events.



## 1 Introduction

30 Under global warming, climate and weather extremes (e.g. flood, drought, heat, wildfire) have increased in the past several decades, and adversely impact the ecosystem and social society (Hao et al., 2018). Drought and heat extremes are among the most devastating climate extremes and influence agriculture, water availability, and the ecosystem (Alizadeh et al., 2020; Hao et al., 2021). Moreover, drought and heat extremes often occur simultaneously or sequentially within a short period, named compound dry and hot events (CDHEs), enhancing the damage caused by individual drought or heat extremes. The evolution  
35 of CDHEs is controlled by synoptic circulation anomalies and local-scale land-atmosphere feedbacks and may cause many other secondary disasters, such as flash droughts, locust plagues, and wildfires (Miralles et al., 2019). CDHEs have received more attention due to their increasing occurrence frequency and intensity over global terrestrial regions (Feng et al., 2020; Geirinhas et al., 2021; Wu et al., 2021a; Wu et al., 2019). Europe has widely been invaded by CDHEs in recent years (Hao et al., 2018; Russo et al., 2019). A significant increasing trend of CDHEs has been reported in the United States (Mazdiyasni  
40 and AghaKouchak, 2015). Meanwhile, some regions of China experienced increasingly severe CDHEs in the last decades, resulting in a massive loss of crop yield (Kong et al., 2020; Lu et al., 2018; Wang and He, 2015).

According to the definition of compound extremes proposed by Zscheischler et al. (2020), CDHEs belong to the category of multivariate compound events. Some studies have investigated CDHEs' evolutions utilizing thresholds to define compound extremes. Beniston (2009) proposed the threshold-based method that classified the joint extremes events as cool/dry,  
45 cool/wet, warm/dry, and warm/wet based on 25% and 75% quantiles. Hao et al. (2013) identified CDHEs based on a threshold of extreme events and found an increasing trend of CDHEs. However, the threshold-based method did not consider other characteristics of the compound events, such as duration and severity, which are of importance for the risk management of extreme climate events. Other joint extremes indices combining drought and hot indices, such as the Standardized Compound Event Indicator (Hao et al., 2019) and Blended Dry and Hot Events Index (Wu et al., 2021a), are  
50 more flexible than the threshold-based indices when analyzing the spatial and temporal characteristics of compound extremes. However, most of the proposed indices are based on monthly meteorological data and can not monitor short-term events timely (e.g., weekly and daily scales).



When extreme high temperature occurs within a short-term period, the evolution of a drought event could be accelerated along with the development of heatwaves (Li et al., 2021; Pendergrass et al., 2020; Yuan et al., 2019). The occurrence of this event may lead to massive crop loss in critical stages of crop growth (e.g. emergence and pollination) (Luan and Vico, 2021). Under climate change, occurrences of such short-term CDHEs have increased and are expected to increase continuously, affecting the ecosystem and society (Luan and Vico, 2021; Zhang et al., 2018). Therefore, it is necessary to develop a short-term time scale index for monitoring the start date, severity, and other characteristics for supporting stakeholders in designing mitigation strategies (Pendergrass et al., 2020). Li et al. (2021) proposed a sub-monthly CDHE index by combining the Standardized Precipitation Evapotranspiration Index (SPEI) and Standardized Temperature Index (STI). This index can monitor short-term SDHEs at sub-monthly scales, considering the influence of different climatic drivers on drought occurrences as it considers atmosphere-land water balance in calculating SPEI with precipitation and potential evapotranspiration (PET) as inputs. To calculate SCDHI, PET was used to represent atmospheric water demand in SPEI, which yet always overestimate droughts, especially in non-arid regions (Ayantobo and Wei, 2019; Zhang et al., 2019a; Zhang et al., 2019b; Zhang et al., 2021b). Feng et al. (2021b) also found the compound dry and hot index by combining SPEI and STI would overestimate CDHEs over global maize areas. Compared to PET, climatically appropriate precipitation for existing conditions ( $\hat{P}$ ), proposed by Palmer (1965) in calculating Palmer Drought Severity Index (PDSI), is a better choice to represent atmospheric water demand. Zhang et al. (2015) proposed a physically based multiscalar drought index (Standardized Moisture Anomaly Index, SZI) at a monthly scale using  $\hat{P}$  in representing atmospheric water demand. Consequently, the SZI was widely used to monitor and project drought evolutions at regional, national, and global scales and displayed better performance in monitoring different categories of droughts (Ayantobo and Wei, 2019; Zhang et al., 2019a; Zhang et al., 2019b; Zhang et al., 2021b).

However, the SZI is incapable of monitoring short-term duration droughts (e.g., days, weeks) as it is calculated based on monthly data. Therefore, this study attempts to expand the time scale of SZI from months to days to evaluate short-term droughts. Consequently, it will be combined with the hot index to construct a compound dry and hot index for investigating important characteristics of CDHEs. The main sections of this paper are as follows: Section 2 introduces Data and Methodology; Section 3 gives validation results of daily SZI and daily compound dry and hot index (DCDHI), and analyses characteristics evolutions in the historical period across non-arid regions of China; Section 4 concludes the main summaries.

## 2 Data and Methodology

### 2.1 Data



In this study, daily gridded meteorological datasets (CN05.1), including precipitation, temperature, humidity, sunshine hours, and wind speed, were used to calculate drought and hot indices. These datasets were provided by the Climate Change Research Centre, Chinese Academy of Sciences (<http://ccrc.iap.ac.cn/resource/detail?id=228>). These data were generated by thin-plate smoothing splines based on over 2,400 stations across China from 1961 to 2021, with a fine spatial resolution of 0.25°×0.25° and high interpolation accuracy (Wu and Gao, 2013; Wu et al., 2017; Xu et al., 2009). This study just focuses on the non-arid regions of China (Fig. 1). The north-western arid regions are not included for the following reasons: The high coverage of desert, little precipitation (about 130 mm/yr), and the melting of glacial and perennially frozen soil contributing to most of the freshwater water make the aridity of the northwest region much higher than other areas so that the calculated index is not comparable. Moreover, the scarce meteorological stations provide insufficient observations that may not produce reliable results.

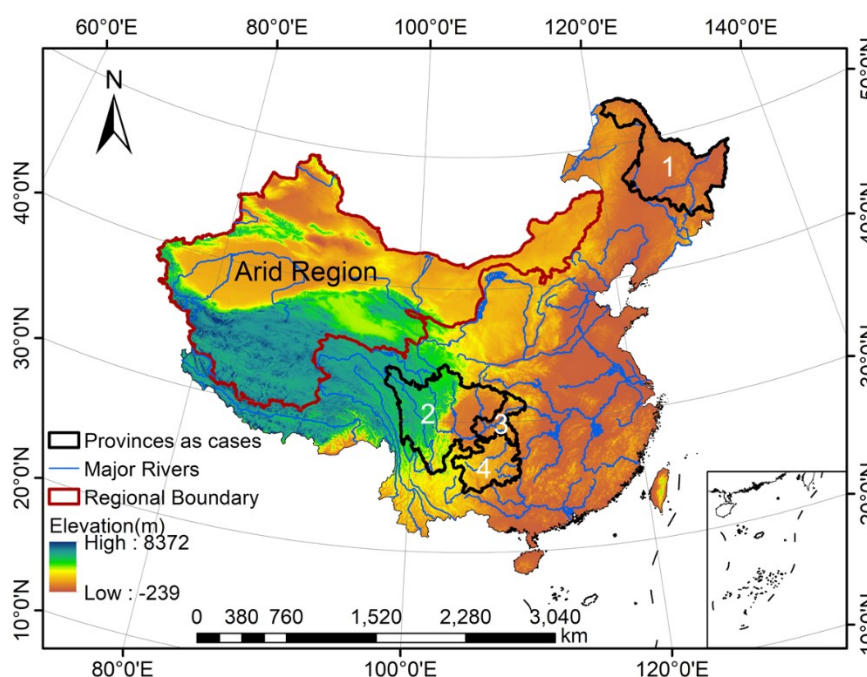


**Figure 1: Digital elevation model of China and provinces as cases in the current study. Note: 1-4 represent Heilongjiang, Sichuan, Chongqing, and Guizhou respectively.**

To evaluate the performance of different drought indices, soil moisture data were also used in the study. Soil moisture is a key component of the water cycle, which controls the water and energy balance and vegetation growth, making it a fundamental indicator for monitoring drought. Soil moisture can be acquired from measurement sites, remote sensing or reanalysis datasets, and land surface or ecohydrological models. Due to the high cost of maintenance, measurement sites are sparsely distributed in most regions, with poor spatial representatives. In contrast, reanalysis and land surface models provide us with continuously spatial and temporal gridded soil moisture, among which NASA Global Land Data



100 Assimilation System Version 2 (GLDAS-2) showed good performances in monitoring wet or dry conditions across China,  
 with a long enough period (Feng et al., 2016; Wu et al., 2021b; Zhang et al., 2021a). The daily GLDAS-2.0 root zone (0~100  
 cm) soil moisture data with  $0.25^\circ \times 0.25^\circ$  resolution were downloaded from the Goddard Earth Sciences Data and Information  
 Services Centre (<https://ldas.gsfc.nasa.gov/gldas>). The root zone soil moisture data were used for the appropriateness in  
 characterizing drought because they have lower noise than land surface soil water (Osman et al., 2021). Then the daily soil  
 105 moisture data were standardized by normal quantile transformation to represent water availability conditions. Additionally,  
 the monthly Normalized Difference Vegetation Index (NDVI) data with 8 km resolution during the period 1981-2015, which  
 represents vegetation conditions, were also collected from the National Tibetan Plateau Third Pole Environment Data Centre  
 (<https://data.tpdc.ac.cn/en/data/9775f2b4-7370-4e5e-a537-3482c9a83d88/>). The NDVI data were bilinearly upscaled into  
 $0.25^\circ \times 0.25^\circ$  resolution and then standardized to NDVI anomalies by subtracting the local mean and dividing by the local  
 110 standard deviation.

## 2.2 Methodology

### 2.2.1 Drought and heat indices

The daily temperature was used to calculate the STI, which was computed according to the fashion of SPI, while not  
 accumulating temperature (McKee et al., 1993; Wang et al., 2021). The probability ( $p$ ) of temperature on each day can be  
 115 calculated by fitting it to a normal distribution as the daily temperature is always assumed normally distributed (Zscheischler  
 et al., 2014). The  $p$  was calculated as follows:

$$p = \frac{1}{\sigma \sqrt{2\pi}} \int_{-\infty}^x \exp\left(-\frac{(x-\mu)^2}{2\sigma^2}\right) dx, \quad (1)$$

where  $x$  represents temperature series,  $\mu$  and  $\sigma$  are mean and standardized deviation, respectively. And then the STI was  
 calculated by standardizing  $p$ .

$$120 \quad STI = \Phi^{-1}(p), \quad (2)$$

PET was estimated using the Penman-Monteith (PM) equation recommended by the Food and Agriculture Organization of  
 the United Nations (FAO) (Allen et al., 1998). The formula of PM is as follows:

$$PET = \frac{0.408 \Delta (R_n - G) + \gamma \frac{900}{T + 273} u_2 (e_s - e_a)}{\Delta + \gamma (1 + 0.34 u_2)}, \quad (3)$$

where  $R_n$  represents surface net radiation ( $\text{MJ m}^{-2} \text{ day}^{-1}$ ),  $G$  represents soil heat flux density ( $\text{MJ m}^{-2} \text{ day}^{-1}$ ),  $T$  represents daily  
 125 air temperature at 2 m height ( $^\circ\text{C}$ ),  $u_2$  represents wind speed at 2 m height ( $\text{m s}^{-1}$ ),  $D$  represents vapor pressure deficit (kPa),



$\Delta$  represents slope vapor pressure curve ( $\text{kPa } ^\circ\text{C}^{-1}$ ), and  $\gamma$  represents psychrometric constant ( $\text{kPa } ^\circ\text{C}^{-1}$ ). The SZI was calculated based on the difference between precipitation and  $\hat{P}$ , where monthly  $\hat{P}$  can be estimated based on surface water balance using four actual variables consisting of evapotranspiration (ET), runoff (RO), loss (L), and recharge (R) and their corresponding potential variables according to PDSI calculation process by dividing soil moisture into 2 layers. The monthly  $\hat{P}_m$  is represented by integrating four potential variables using weighting factors at each month ( $\alpha, \beta, \gamma$ , and  $\delta$ ):

$$\hat{P}_m = \alpha_j PET + \beta_j PR + \gamma_j PRO - \delta_j PL, j = 1, 2, 3, \dots, 12, \quad (4)$$

The weighting factors are named water-balance coefficients, calculated as follows:

$$\alpha_j = \frac{\overline{ET}_j}{\overline{PET}_j}, \beta_j = \frac{\overline{R}_j}{\overline{PR}_j}, \gamma_j = \frac{\overline{RO}_j}{\overline{PRO}_j}, \delta_j = \frac{\overline{L}_j}{\overline{PL}_j}, \quad (5)$$

where  $j$  represents calendar months, and bar represents mean values. For more details on the calculation of these factors, one can refer to Wells et al. (2004). The daily  $\hat{P}_d$  can be calculated by dividing  $\hat{P}_m$  using the number of days in the  $j$ th month ( $d_j$ ).

$$\hat{P}_d = \frac{\hat{P}_m}{d_j}, \quad (6)$$

Then the daily difference between precipitation ( $P$ ) and  $\hat{P}_d$  was calculated for representing water balance. To reflect drought conditions on a specific day, the antecedent water surplus or deficit (WSD) was computed as follows:

$$WSD = \sum_{i=1}^n (P - \hat{P}_d)_i, \quad (7)$$

where  $n$  represents the number of previous days before the current day. The WSD can be aggregated at arbitrary time scales, such as a week, a month, 3 months, or seasons. The WSD was then fitted by a log-logistic cumulative distribution ( $p$ ). Lastly, the daily SZI was obtained by standardizing  $p$  as Eq (2).

$$p = P(D) = \left[ 1 + \left( \frac{\alpha}{D - \gamma} \right)^\beta \right]^{-1}, \quad (8)$$

In addition, two commonly used drought indices (SPI and SPEI) were also used in comparison with SZI. The calculation steps of these indices can be found in Li et al. (2020), McKee et al. (1993), Vicente-Serrano et al. (2010), and Wang et al. (2021).



### 2.2.2 Construction of compound dry and hot index

The DCDHI was constructed by linking SZI and STI using the Copula function, which was a multivariate cumulative distribution function describing the dependence between random variables. In this study, Frank copula, one of Archimedean copulas, was used to joint SZI and STI for it has good performance for hydrometeorological variables (Ayantobo et al., 2019; Feng et al., 2021a; Li et al., 2021). The compound dry and hot event was identified when the temperature was less than a threshold value and WSD was higher than a threshold. Let  $X$  and  $Y$  represent WSD and temperature respectively, and the cumulative joint probability was calculated as follows:

$$p = P(X < x, Y > y) = u - c(u, v), \quad (9)$$

where  $u$  and  $v$  are thresholds after uniform transformed  $X$  and  $Y$ , and  $c(u, v)$  represents the joint probability of  $u$  and  $v$  linked by Frank copula. Then the DCDHI was calculated by transforming  $p$  using the inverse normal distribution. The negative DCDHI represents occurrences of compound dry and hot events. According to the recommendation of Wu et al. (2020), five categories of dry and hot conditions were defined, consisting of abnormal, light, moderate, heavy, and extreme conditions, shown in Table 1.

$$DCDHI = \phi^{-1} \left( F \left( P(X < x, Y > y) \right) \right), \quad (10)$$

**Table 1.** Categories of compound dry and hot events.

Categories	Dry-hot conditions	DCDHI
C1	Abnormal	$(-0.80, -0.50]$
C2	Light	$(-1.30, -0.80]$
C3	Moderate	$(-1.60, -1.30]$
C4	Heavy	$(-2.0, -1.60]$
C5	Extreme	$\leq -2.0$

### 2.2.3 Extraction of compound characteristics

The run theory was used in this study to extract compound characteristics, including frequency, duration, severity, and intensity of the CDHEs. A ‘run’ was defined when DCDHI was less than the truncation level ( $X_0$ ) over a continuous period (Fig. 2). Next, the frequency (F), duration (D), severity (S), and Intensity (I) were extracted. The definitions of these characteristics can be found in Ayantobo et al. (2017) and Mishra and Singh (2010). The number of continuous days when DCDHI was below  $X_0$  was defined as  $D$ , and the cumulative sum of DCDHI values during a CDHE event was defined as  $S$ . For comparison with other characteristics,  $S$  was inverted to a positive number.





$$D = t_e - t_s, \quad (11)$$

$$S = - \sum_{t=1}^n DCDHI_t, \quad (12)$$

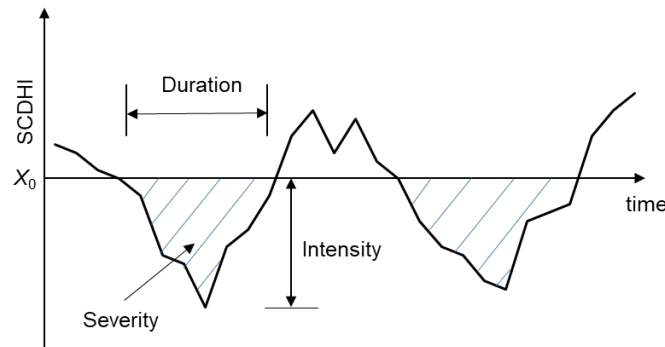


Figure 2: Schematic diagram of the run theory.  $X_0$  is the threshold, and CDHE occurs when DCDHI is less than  $X_0$ .

## 175 3 Results and Discussion

### 3.1 Evaluation of daily SZI in drought monitoring

The DCDHI was constructed based on daily SZI and STI, so it was necessary to evaluate the performance of daily SZI in drought monitoring at multiple timescales. Fig. 3 shows the spatial distributions of correlations between soil moisture and daily SPI, SPEI, and SZI at multiple time scales (1-, 3-, 6-, 9-, and 12-month). For daily indices at 1-month and 3-month scales, correlations between SPI and soil moisture (SM), SPEI-SM, and SZI-SM decrease gradually from South to North, which means these indices perform better in warm and humid regions than that in cold regions (Fig. 3). The correlations in Fig. 4 for SZI-SM (averaged  $r = 0.43$  at 1-month scale, averaged  $r = 0.58$  at 3-month scale) are higher than that for SPI-SM (averaged  $r = 0.25$  at 1-month scale, averaged  $r = 0.42$  at 3-month scale) and SPEI-SM (averaged  $r = 0.29$  at 1-month scale, averaged  $r = 0.47$  at 3-month scale). SZI correlates better with SM in northern cold and non-humid regions than SPEI, indicating SZI can better monitor drought across different climatic regions. At 6-month scale, the correlations for SPI-SM and SPEI-SM are lower in the South than that at 1-month and 3-month scales. In contrast, the correlations are higher in the North than that at short time scales. The distribution for SZI-SM at 6-month scale shows a similar pattern to that at 3-month scale, with an average value of 0.64 (Fig. 4). At longer time scales (9 and 12 months), correlations for SPI-SM, SPEI-SM, and SZI-SM are higher in the North than that in the South. In a word, the daily SZI is a reliable indicator in monitoring drought at different time scales, and SZI at 3-, 6-, and 9-month scales can better monitor agricultural drought than SPI and SPEI (represented by soil moisture).



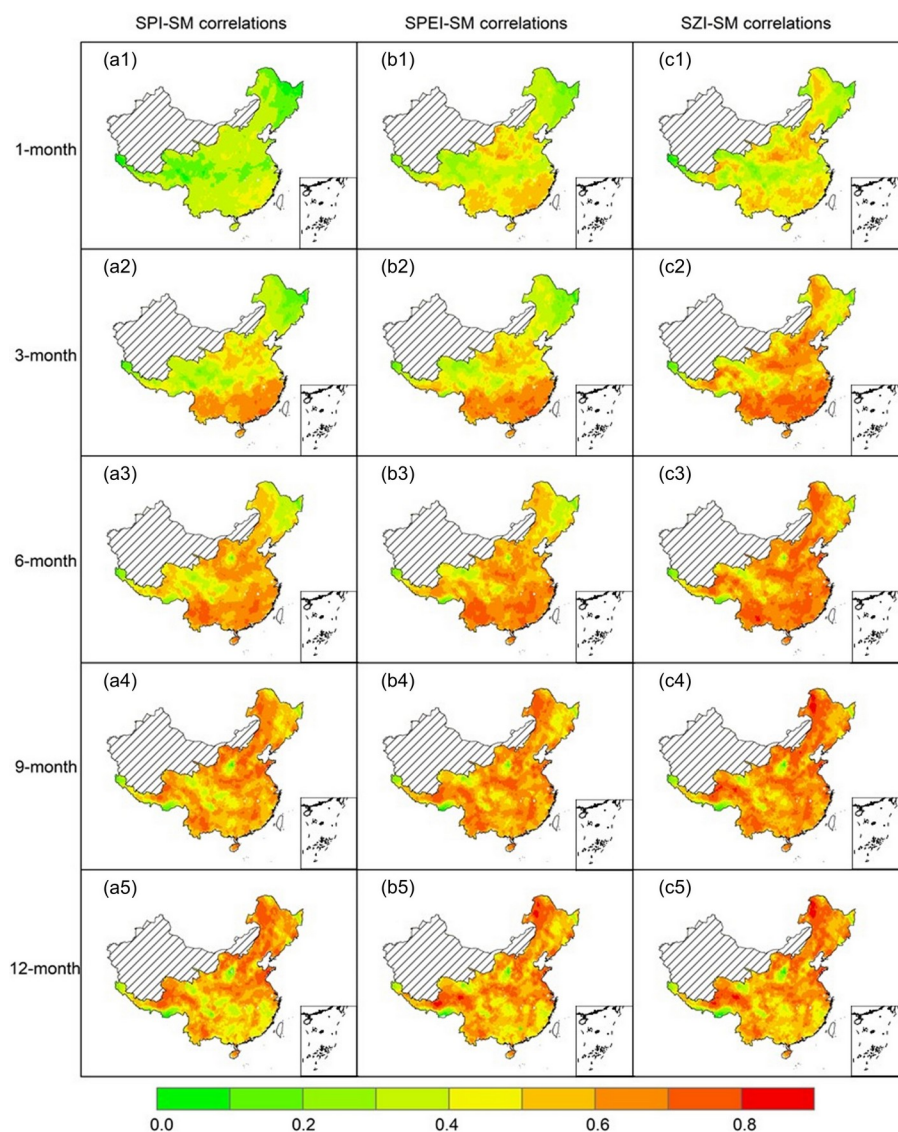


**Figure 3: Spatial distributions of correlations between SSMI and SPI, SPEI, and SZI at 1-, 3-, 6-, 9-, and 12-month scales.**

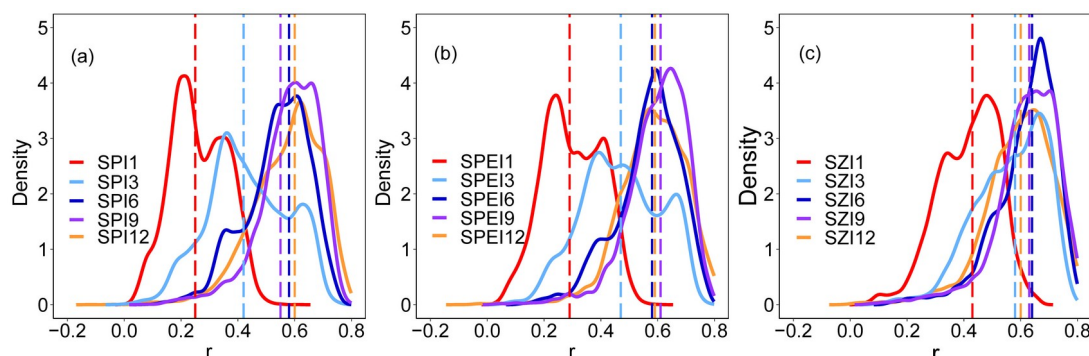


**Figure 4: The density of correlations between SM and (a) SPI, (b) SPEI, and (c) SZI at 1-, 3-, 6-, 9- and 12-month scales.**

To further evaluate the performance of the daily SZI in drought monitoring, two actual drought events were selected as case studies. Southwestern China with a humid climate (Guizhou, Yunnan, Guangxi, and Sichuan provinces, shown in Fig. 1) suffered severe drought from the autumn of 2009 to the summer of 2010. This study selected drought events that occurred in Guizhou province as the first case. Fig. 5a shows the variations of daily SZI at 1-month, 3-month, and 6-month scales and soil moisture from 1st July, 2009 to 31st July, 2010. The drought started in September of 2009 and became worse and spread in the winter of 2009 and spring of 2010, lasting about 8 months. Afterward, the drought was relieved at the end of May, 2010, and ended in early July, 2010.

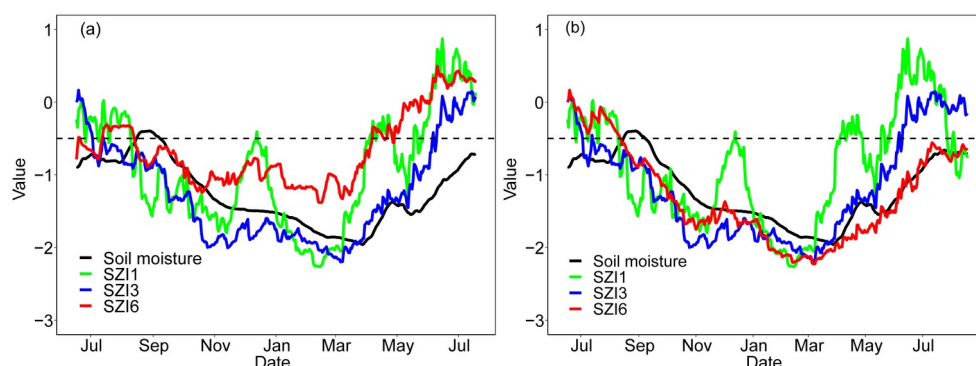


**Figure 5: Daily SZI and standardized soil moisture (a) during 2009-2010 in Guizhou province and (b) Heilongjiang province. Note: the dashed black line is the drought threshold at -0.5, below which drought occurs.**

Coincidentally, north-eastern China with a cold climate was also attacked by drought from 2009 to 2010, and the drought event that occurred in Heilongjiang province (shown in Fig.1) was selected as the second case (Fig. 5b). The drought started at the end of July 2009 and intensified in September, lasting for 9 months. Finally, the drought was relieved and disappeared in late July. For the drought in Guizhou province, variation of soil moisture agrees better with SZI3 than with SZI1 and SZI6, also indicating the good performance of SZI3 in monitoring agricultural drought in humid regions as shown in Fig. 3. In contrast, SZI6 performs better in Heilongjiang province as shown in Fig. 3. Water cycle speed is slower in cold regions due to the existence of frozen soil and glaciers than that in warm regions, which makes soil moisture a longer memory.



Therefore, soil moisture variations in these regions show a better consistency with longer time scales SZI. Overall, like daily SPI and daily SPEI, daily SZI could monitor drought at multiple time scales and is more sensitive to soil moisture variations.

215 The daily SZI is superior in monitoring both short-term and long-term droughts and can be applied to detect flash drought which occurs more frequently and severely with climate warming.

### 3.2 Evaluation of the DCDHI

Given the better performance of SZI in drought monitoring, it is joined with STI through the copula method to construct DCDHI for identifying CDHEs. Though the copula has been commonly used in connecting two different marginal distributions of meteorological or hydrological variables, it is the first time to link daily SZI and STI. Therefore, it is necessary to test the applicability of daily DCDHI in monitoring CDHEs. Fig. 6 shows correlation patterns between DCDHI and SZI/STI at different time scales. DCDHI correlated significantly ( $p < 0.01$ ) with SZI over non-arid regions of China, with average correlation coefficients of 0.75, 0.72, and 0.71 at 3, 6, and 9-month scales, respectively. DCDHI shows a strong negative correlation ( $p < 0.01$ ) with STI, with average correlations of -0.78, -0.75, -0.73 at 3-, 6-, and 9-month scales, respectively.

225 Overall, DCDHI agrees well with drought and heat indices, demonstrating its applicability in detecting dry and hot events.

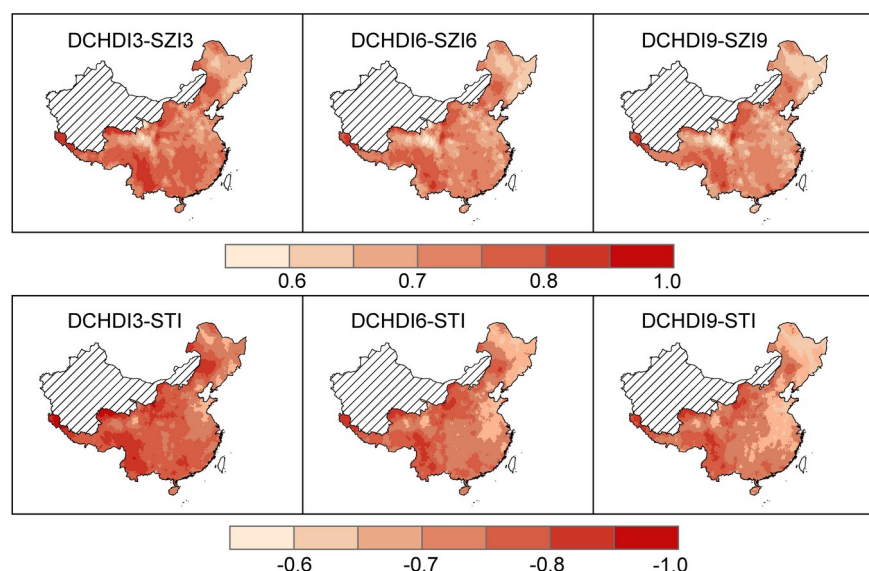
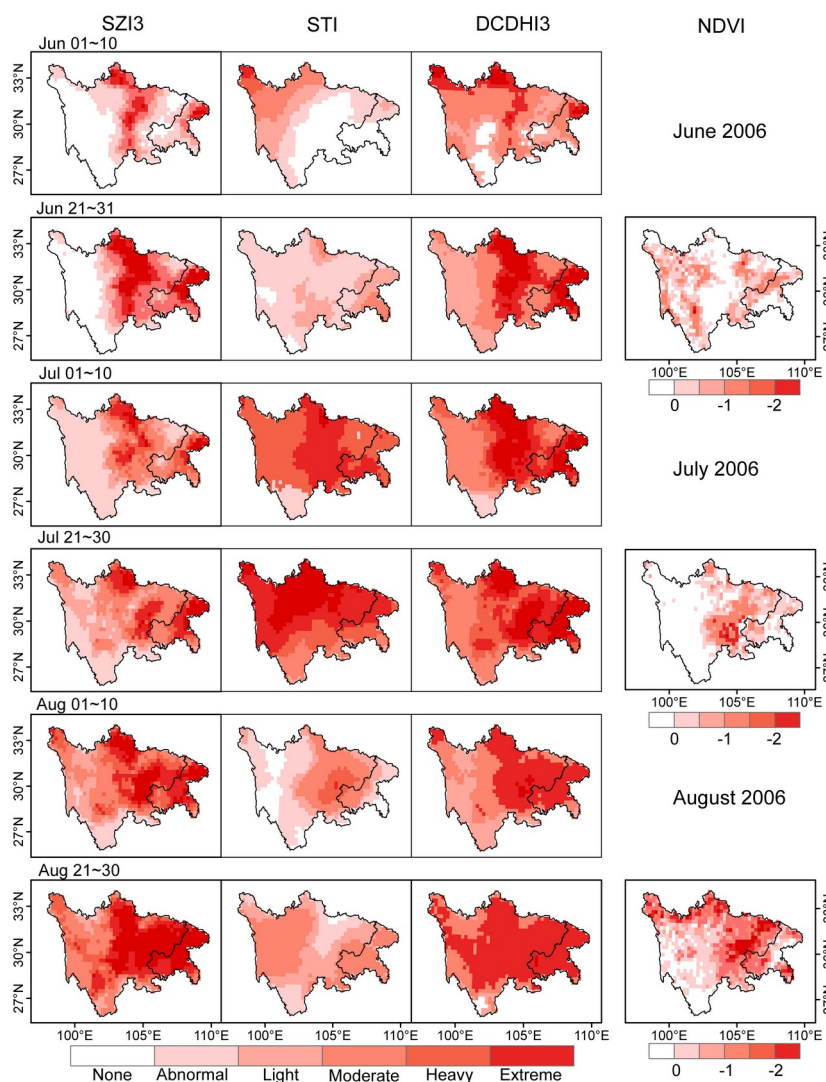


**Figure 6: Spatial patterns of correlations between DCDHI and SZI/STI at 3-, 6-, and 9-month scales.**

To further test the applicability of the DCDHI in detecting CDHEs, an extreme drought accompanied by the heatwave event that occurred during the summer of 2006 in southwestern China was selected as a case. The average summer precipitation in Sichuan province and Chongqing municipality was 345.9 mm, only 67% of the same period of the year, which is the lowest value in the same period in history since 1951. The average temperature in summer 2006 (June-August) in Sichuan-Chongqing hit the highest level since 1951. The long duration and intensity of high-temperature days in some areas of

Sichuan-Chongqing have all set historical extremes for the same period on record. This unprecedented CDHE event caused adverse impacts on society and the ecosystem (Wang et al., 2015; Wu et al., 2020). Fig. 7 shows the spatial patterns of SZI3, STI, DCDHI3, and the corresponding impact on vegetation (NDVI) during the summer of 2006 at the decade scale. The event started in early June of 2006 and expanded throughout the entire Sichuan-Chongqing region in late June. In July of 2006, most regions of Sichuan-Chongqing were attacked by the moderate to extreme hot events, and the eastern Sichuan-Chongqing was also hit by heavy drought events, causing extreme CDHEs. During this period, CDHEs affected vegetation growth and caused negative NDVI anomalies in some CDHEs affected regions. In late August, the CDHEs were more severe with extreme drought events, causing a larger area of negative NDVI anomalies. Overall, the CDHEs identified by the DCDHI are consistent with records in some published documents (<http://www.weather.com.cn>) and NDVI variations, demonstrating the robustness and capability of the DCDHI in monitoring CDHEs at a sub-monthly scale.



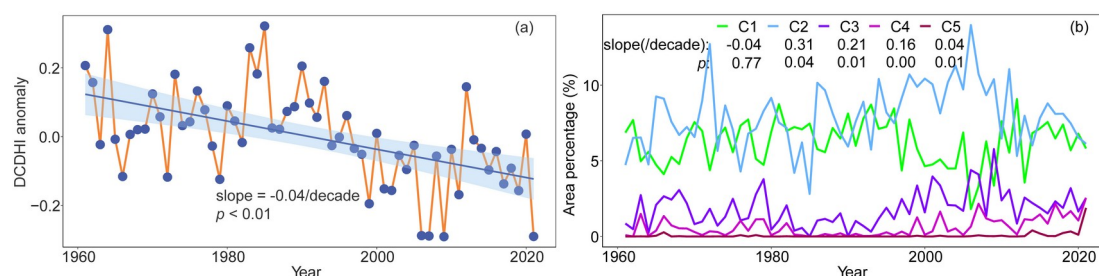




245 **Figure 7: Evolutions of droughts, heatwaves, CDHEs, and vegetation conditions represented by SZI3, STI, DCDHI3, and NDVI anomalies respectively.**

### 3.3 Variations of different characteristics

CDHEs occurred during the growing seasons of crops (April–September) were selected. Only CDHEs that persist for more than a week are selected for characteristics analysis because short-term CDHEs often last at least several days (Otkin et al., 2018). Fig. 8 shows the variations of the 3-month scale DCDHI and the area percentage affected by different CDHE severity categories (C1–C5) during the period 1961–2021. DCDHI shows a significant declining trend ( $-0.04/\text{decade}$ ), demonstrating exacerbated CDHEs with global warming (Fig. 8a). There was also a significant increasing trend in the area affected by light, moderate, heavy, and extreme CDHEs, with increasing slopes of 0.31, 0.21, 0.16, and 0.04 respectively (Fig. 8b).



255 **Figure 8: Variations of average DCDHI at a 3-month scale and area percentage affected by different categories of CDHEs during 1961–2021.**

In recent decades, the temperature increased rapidly along with the high emission of greenhouse gas, especially after 1990. The increasing rate of temperature during 1990–2021 is about  $0.32\text{ }^{\circ}\text{C}/\text{decade}$ , much higher than that during 1961–1989 ( $0.08\text{ }^{\circ}\text{C}/\text{decade}$ ) (Fig. 9). To assess the spatial variations of CDHEs, spatial patterns of different characteristics in 1961–1989 and 1990–2021 were compared to explore the response of CDHEs to global warming. Fig. 10 shows the spatial patterns of different characteristics for 1961–1989 and 1990–2021 periods, using  $-0.8$  as the run theory threshold (Li et al., 2021). Higher frequency and intensity of CDHEs are detected for 1990–2021 than that for 1961–1989. In contrast, the duration and severity in 1990–2021 are shorter and lower in most eastern regions than that in 1989–2021. Southwestern regions of China show an obvious increase in duration, severity, and intensity from 1961–1989 to 1990–2021. The duration is longer than 30 days, and the severity is larger than 70 in some regions of the southwest for 1990–2021, which shows a reverse pattern to that for 1961–1989. The increased CDHEs in southwestern regions of China have also been found in previous studies (Wu et al., 2019; Wu et al., 2020).

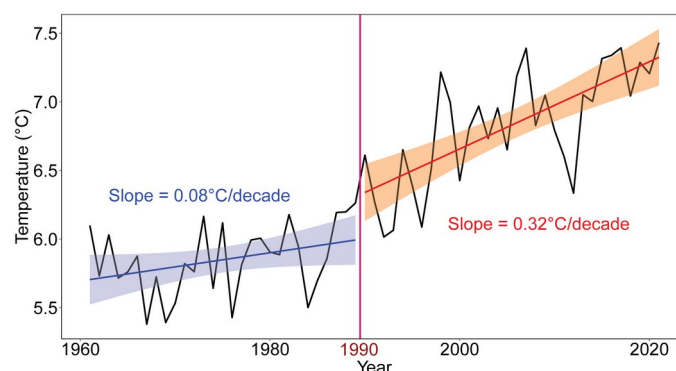


**Figure 9: Annual temperature variation averaged over non-arid regions of China from 1961 to 2021.**

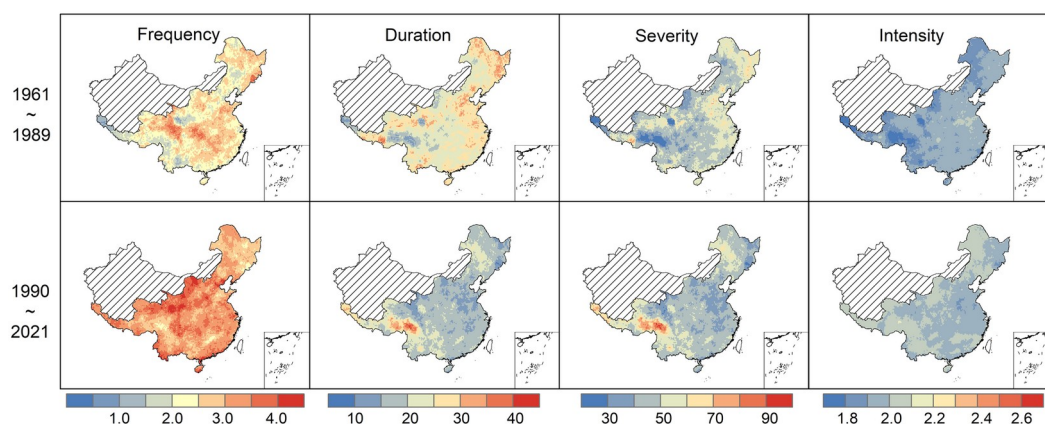


**Figure 10: The spatial patterns of characteristics (frequency, duration, severity, and intensity) of CDHEs for the periods of 1961-1989 and 1990-2021 respectively, using -0.8 as the run theory threshold. Note: frequency indicates the annual average number of events.**

Given the destructive impacts of severe CDHEs, the spatial difference among characteristics using -2.0 as the run theory threshold were compared (Fig. 11). It can be found that frequency and duration decreased, while intensity increased in most regions from -0.8 to -2.0 thresholds. CDHEs occurred more frequently for the period 1990-2021 (occurring once to twice per year) than 1961-1989 (lower than once per year). The severity decreased from the period 1961-1989 to 1990-2021 in northern regions but increased in southern especially southwestern regions, similar to that with -0.8 as a threshold value. Moreover, the intensity of CDHEs also shows an obvious increase from 1961-1989 to 1990-2021, which indicates that intensified extreme CDHEs are more likely to occur with global warming, affecting grain production.

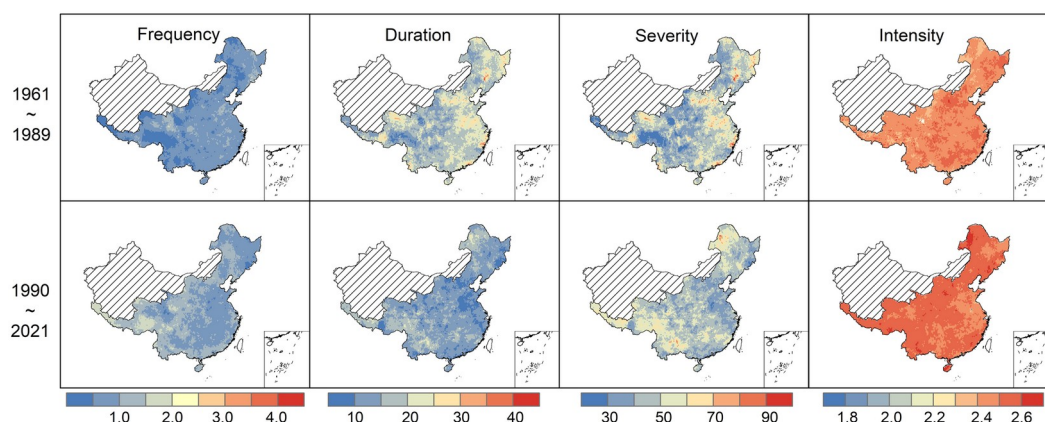


**Figure 11: As Fig. 10, but using -2.0 as the run theory threshold.**

Overall, DCDHI shows a significant decreasing trend with an obvious temperature increase in almost all regions of China (Fig. 12). Shorter duration and intensified CDHEs occurred more frequently for the period 1990-2021, especially in southwestern regions of China, where soil moisture is almost not limiting and the evapotranspiration is dominated by solar radiation. Under global warming, higher radiation and temperature accelerated the evapotranspiration process and deplete soil moisture more quickly, which leads to short-term droughts. Simultaneously, global warming increased occurrences of consecutive extreme heat events, which can increase soil moisture loss in a short period and intensify drought conditions (Zhang et al., 2018). Moreover, these regions are covered by dense vegetation, which would absorb more water from the soil to guarantee the respiration process when the temperature is high, accelerating evapotranspiration and soil moisture loss (Li et al., 2020; Li et al., 2021). Consequently, latent heat would decrease due to the soil water deficit, and sensible heat (temperature) would increase, leading to a higher temperature. The higher temperature would increase atmospheric vapor pressure deficit, which would in turn exacerbate soil moisture depletion and enhance drought (Zhou et al., 2019). Therefore, the land-atmospheric feedback facilitates the occurrence of CDHEs. Precipitation shows a decreasing trend in some regions of southwestern China, which has also intensified drought conditions (Fig. 12). In addition, vegetation greening has also accelerated evapotranspiration and reduced water yield, leading to more severe droughts (Bai et al., 2020).

The increased CDHEs and their different characteristics are caused by various factors as mentioned above, including temperature and precipitation variations, changed precipitation-temperature dependence, which is attributed to the background warming (due to higher emissions of greenhouse gas), land surface-atmosphere feedbacks, sea surface temperature anomalies, atmospheric circulation anomalies, and so on (Cheng et al., 2019; Feng et al., 2020; Zscheischler et al., 2020; Zscheischler et al., 2018). The driving mechanisms (dynamic and thermodynamic) of CDHEs, beyond the scope of this study, will be investigated in future research.



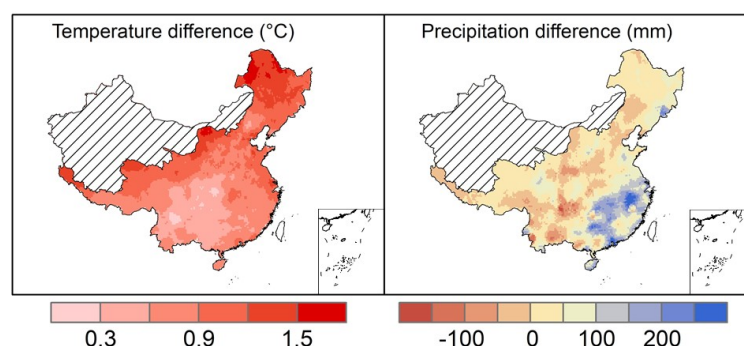


**Figure 12: Annual temperature and precipitation differences between 1961-1989 and 1990-2021 periods.**

## 305 4 Conclusions

Global warming enhanced short-term drought and heat extremes, causing substantial damage when they occurred in the key stages of crop growth. An accurate daily scale compound dry and hot index is necessary for reflecting evolutions of short-term dry and hot conditions, which can provide timely warnings for stakeholders. This study first expanded the time scale of the Standardized Moisture Anomaly Index (SZI) from months to days for evaluating short-term droughts. Then, it was combined with the hot index to construct a daily scale compound dry and hot (DCDHI) index using Copula theory for investigating important characteristics of compound dry and hot events. The applicability of daily SZI and DCDHI indices in monitoring short-term and long-term drought and compound dry and hot events was verified across non-arid regions of China. The frequency, duration, severity, and intensity of compound dry and hot events during growing seasons (April to October) were also investigated from 1961 to 2021. The key summaries of the study are as follows: The daily SZI agrees better with soil moisture variations than SPI and SPEI at different time scales, indicating that SZI is superior in monitoring both short-term and persistent droughts and can be applied to construct daily DCDHI for detecting short-term dry and hot events. DCDHI can well capture spatial evolutions of droughts and heats at a daily scale, and well reflect vegetation losses. Therefore, DCDHI is a good indicator for detecting compound dry and hot events at different time scales (daily to monthly). From 1961 to 2021, DCDHI shows a significant declining trend ( $-0.04/\text{decade}$ ), indicating compound dry and hot events increased during this period. There exists a significant increase in the area affected by light, moderate, heavy, and extreme compound dry and hot events, with increasing slopes of 0.31, 0.21, 0.16, and 0.04 respectively. Compound dry and hot events occurred more frequently for the period 1990-2021 than 1961-1989. The severity decreased from the period 1961-1989 to 1990-2021 in northern regions but increased in southern especially southwestern regions. More intensified compound dry and hot events are more likely to occur with global warming, which could cause more devastating impacts on crop production. In a word, this study proposes a new tool for detecting evolutions and characteristics of short-term compound dry and hot events, which can provide useful insights for understanding short-term compound dry and hot events and valuable information timely for stakeholders.



*Data availability.* The gridded meteorological data are downloaded from the Climate Change Research Centre, Chinese Academy of Sciences (<http://ccrc.iap.ac.cn/resource/detail?id=228>). The soil moisture data are downloaded from the Goddard Earth Sciences Data and Information Services Centre (<https://ldas.gsfc.nasa.gov/gldas>). The NDVI data are obtained from the National Tibetan Plateau Third Pole Environment Data Centre (<https://data.tpdc.ac.cn/en/data/9775f2b4-7370-4e5e-a537-3482c9a83d88/>). Daily PET, SZI, SPI, SPEI, and DCDHI and their corresponding R codes are provided for requests by contacting corresponding authors.

*Author contributions.* HW, GZ, XS, and XF designed the experiment, analyzed the data, and wrote the manuscript. SZ, SS, LS, and KF edited and revised the paper.

*Competing interests.* The authors declare no competing interests.

*Acknowledgments.* This study is funded by the National Natural Science Foundation of China (Grant No. 51709046); the Lanzhou Institute of Arid Meteorology (Grant No. IAM202119). We thank the data providers mentioned in Section 2.1.



## 340 References

- Alizadeh, M. R., Adamowski, J., Nikoo, M. R., AghaKouchak, A., Dennison, P., and Sadegh, M.: A century of observations reveals increasing likelihood of continental-scale compound dry-hot extremes, *Science Advances*, 6, eaaz4571, DOI: 10.1126/sciadv.aaz4571, 2020.
- Allen, R. G., Pereira, L. S., Raes, D., and Smith, M.: Crop evapotranspiration, guidelines for computing crop water requirements. FAO Irrigation and Drainage Paper 56. Food and Agriculture Organization of the United Nations, Rome, Italy.
- 345 Ayantobo, O. O., Li, Y., and Song, S.: Multivariate drought frequency analysis using four-variate symmetric and asymmetric Archimedean copula functions, *Water Resources Management*, 33(1), 103–127, DOI: 10.1007/s11269-018-2090-6, 2019.
- Ayantobo, O. O., Li, Y., Song, S., and Yao, N.: Spatial comparability of drought characteristics and related return periods in  
 350 mainland China over 1961–2013, *Journal of Hydrology*, 550, 549–567, DOI: 10.1016/j.jhydrol.2017.05.019, 2017.
- Ayantobo, O. O., and Wei, J.: Appraising regional multi-category and multi-scalar drought monitoring using standardized moisture anomaly index (SZI): A water-energy balance approach, *Journal of Hydrology*, 579, 124–139, DOI: 10.1016/j.jhydrol.2019.124139, 2019.
- Bai, P., Liu, X., Zhang, Y., and Liu, C.: Assessing the impacts of vegetation greenness change on evapotranspiration and  
 355 water yield in China, *Water Resources Research*, 56, e2019WR027019, DOI: 10.1029/2019WR027019, 2020.
- Beniston, M.: Trends in joint quantiles of temperature and precipitation in Europe since 1901 and projected for 2100, *Geophysical Research Letters*, 36(7), L07707, DOI: 10.1029/2008gl037119, 2009.
- Cheng, L., Hoerling, M., Liu, Z., and Eischeid, J.: Physical understanding of human-induced changes in U.S. hot droughts using equilibrium climate simulations, *Journal of Climate*, 32(14), 4431–4443, DOI: 10.1175/jcli-d-18-0611.1, 2019.
- 360 Feng, K., Su, X., Singh, V. P., Ayantobo, O. O., Zhang, G., Wu, H., and Zhang, Z.: Dynamic evolution and frequency analysis of hydrological drought from a three-dimensional perspective, *Journal of Hydrology*, 600, 126675, DOI: 10.1016/j.jhydrol.2021.126675, 2021a.
- Feng, S., Hao, Z., Wu, X., Zhang, X., and Hao, F.: A multi-index evaluation of changes in compound dry and hot events of global maize areas, *Journal of Hydrology*, 602, 126728, DOI: 10.1016/j.jhydrol.2021.126728, 2021b.
- 365 Feng, S., Wu, X., Hao, Z., Hao, Y., Zhang, X., and Hao, F.: A database for characteristics and variations of global compound dry and hot events, *Weather and Climate Extremes*, 30, 100299, DOI: 10.1016/j.wace.2020.100299, 2020.
- Feng, X., Fu, B., Piao, S., Wang, S., Ciais, P., Zeng, Z., ... and Wu, B.: Revegetation in China's Loess Plateau is approaching sustainable water resource limits, *Nature Climate Change*, 6(11), 1019–1022, DOI: 10.1038/nclimate3092, 2016.



- 370 Geirinhas, J. L., Russo, A., Libonati, R., Sousa, P. M., Miralles, D. G., and Trigo, R. M.: Recent increasing frequency of compound summer drought and heatwaves in Southeast Brazil, *Environmental Research Letters*, 16, 034036, DOI: 10.1088/1748-9326/abe0eb, 2021.
- Hao, Y., Hao, Z., Fu, Y., Feng, S., Zhang, X., Wu, X., and Hao, F.: Probabilistic assessments of the impacts of compound dry and hot events on global vegetation during growing seasons, *Environmental Research Letters*, 16, 074055, DOI: 10.1088/1748-9326/ac1015, 2021.
- 375 Hao, Z., Hao, F., Singh, V. P., and Zhang, X.: Changes in the severity of compound drought and hot extremes over global land areas, *Environmental Research Letters*, 13, 124022, DOI: 10.1088/1748-9326/aaee96, 2018.
- Hao, Z., Hao, F., Singh, V. P., and Zhang, X.: Statistical prediction of the severity of compound dry-hot events based on El Niño-Southern Oscillation, *Journal of Hydrology*, 572, 243–250, DOI: 10.1016/j.jhydrol.2019.03.001, 2019.
- 380 Kong, Q., Guerreiro, S. B., Blenkinsop, S., Li, X. F., and Fowler, H. J.: Increases in summertime concurrent drought and heatwave in Eastern China, *Weather and Climate Extremes*, 28, 100242, DOI: 10.1016/j.wace.2019.100242, 2020.
- Li, J., Wang, Z., Wu, X., Xu, C., Guo, S., and Chen, X.: Toward monitoring short-term droughts using a novel daily scale, standardized antecedent precipitation evapotranspiration index, *Journal of Hydrometeorology*, 21(5), 891–908, DOI: 10.1175/jhm-d-19-0298.1, 2020.
- 385 Li, J., Wang, Z., Wu, X., Zscheischler, J., Guo, S., and Chen, X.: A standardized index for assessing sub-monthly compound dry and hot conditions with application in China, *Hydrology and Earth System Sciences*, 25(3), 1587–1601, DOI: 10.5194/hess-25-1587-2021, 2021.
- Lu, Y., Hu, H., Li, C., and Tian, F.: Increasing compound events of extreme hot and dry days during growing seasons of wheat and maize in China, *Scientific Reports*, 8(1), 16700, DOI: 10.1038/s41598-018-34215-y, 2018.
- 390 Luan, X., and Vico, G.: Canopy temperature and heat stress are increased by compound high air temperature and water stress and reduced by irrigation - a modeling analysis, *Hydrology and Earth System Sciences*, 25(3), 1411–1423, DOI: 10.5194/hess-25-1411-2021, 2021.
- Mazdiyasni, O., and AghaKouchak, A.: Substantial increase in concurrent droughts and heatwaves in the United States, *Proceedings of the National Academy of Sciences*, 112(37), 11484–11489, DOI: 10.1073/pnas.1422945112, 2015.
- 395 Mckee, T. B., Doesken, N. J., and Kleist, J.: The relationship of drought frequency and duration to time scales, *Eighth Conference on Applied Climatology American Meteorology Society, Anaheim*, pp. 17–22, 1993.
- Mishra, A. K., and Singh, V. P.: A review of drought concepts, *Journal of Hydrology*, 391(1–2), 202–216, DOI: 10.1016/j.jhydrol.2010.07.012, 2010.
- Osman, M., Zaitchik, B. F., Badr, H. S., Christian, J. I., Tadesse, T., Otkin, J. A., and Anderson, M. C.: Flash drought onset over the contiguous United States: sensitivity of inventories and trends to quantitative definitions, *Hydrology and Earth System Sciences*, 25(2), 565–581, DOI: 10.5194/hess-25-565-2021, 2021.
- 400



- Otkin, J.A., Svoboda, M., Hunt, E. D., Ford, T. W., Anderson, M. C., Hain, C., and Basara, J. B.: Flash droughts: A review and assessment of the challenges imposed by rapid-onset droughts in the United States, *Bulletin of the American Meteorological Society*, 99(5), 911–919, DOI: 10.1175/bams-d-17-0149.1, 2018.
- 405 Palmer, W.C.: Meteorological drought, US department of commerce, Weather Bureau, Washington, DC, 58, 1965.
- Pendergrass, A. G., Meehl, G. A., Pulwarty, R., Hobbins, M., Hoell, A., AghaKouchak, A., ... and Woodhouse, C. A.: Flash droughts present a new challenge for subseasonal-to-seasonal prediction, *Nature Climate Change*, 10(3), 191–199, DOI: 10.1038/s41558-020-0709-0, 2020.
- Russo, A., Gouveia, C.M., Dutra, E., Soares, P.M.M., and Trigo, R.M.: The synergy between drought and extremely hot  
 410 summers in the Mediterranean, *Environmental Research Letters*, 14, 014011, DOI: 10.1088/1748-9326/aaf09e, 2019.
- Vicente-Serrano, S. M., Beguería, S., and López-Moreno, J. I.: A multiscale drought index sensitive to global warming: The Standardized Precipitation Evapotranspiration Index, *Journal of Climate*, 23(7), 1696–1718, DOI: 10.1175/2009jcli2909.1, 2010.
- Wang, H., and He, S.: The North China/Northeastern Asia severe summer drought in 2014, *Journal of Climate*, 28(17),  
 415 6667–6681, DOI: 10.1175/jcli-d-15-0202.1, 2015.
- Wang, L., Chen, W., Zhou, W., and Huang, G.: Drought in Southwest China: A review, *atmospheric and oceanic science Letters*, 8(6), 339–344, DOI: 10.3878/AOSL20150043, 2015.
- Wang, Q., Zhang, R., Qu, Y., Zeng, J., Wu, X., Zhou, X., ... and Zhou, D.: Daily standardized precipitation index with multiple time scale for monitoring water deficit across the mainland China from 1961 to 2018, *Earth System Science*  
 420 Data Discuss [preprint], DOI: 10.5194/essd-2021-105, 2021.
- Wells, N., Goddard, S., and Michaelsen, J.: A self-calibrating Palmer Drought Severity Index, *Journal of Climate*, 17, 2335–2351, 2004.
- Wu, H., Su, X., and Singh, V.P.: Blended dry and hot events index for monitoring dry-hot events over global land areas, *Geophysical Research Letters*, 48, e2021GL096181, DOI: 10.1029/2021gl096181, 2021a.
- 425 Wu, J., and Gao, X.: A gridded daily observation dataset over China region and comparison with the other datasets, *Chinese Journal of Geophysics*, 56(4), 1102–1111, DOI: /10.6038g20130406, 2013.
- Wu, J., Gao, X., Giorgi, F., and Chen, D.: Changes of effective temperature and cold/hot days in late decades over China based on a high resolution gridded observation dataset, *International Journal of Climatology*, 37(S1), 788–800, DOI: /10.1002/joc.5038, 2017.
- 430 Wu, X., Hao, Z., Hao, F., and Zhang, X.: Variations of compound precipitation and temperature extremes in China during 1961–2014, *Science of the Total Environment*, 663, 731–737, DOI: 10.1016/j.scitotenv.2019.01.366, 2019.
- Wu, X., Hao, Z., Zhang, X., Li, C., and Hao, F.: Evaluation of severity changes of compound dry and hot events in China based on a multivariate multi-index approach, *Journal of Hydrology*, 583: 124580, DOI: 10.1016/j.jhydrol.2020.124580, 2020.



- 435 Wu, Z., Feng, H., He, H., Zhou, J., and Zhang, Y.: Evaluation of soil moisture climatology and anomaly components derived from ERA5-Land and GLDAS-2.1 in China, *Water Resources Management*, 35(2), 629–643, DOI: 10.1007/s11269-020-02743-w, 2021b.
- Xu, Y., Guo, X., Shen, Y., Xu, C., Shi, Y., and Giorgi, F.: A daily temperature dataset over China and its application in validating a RCM simulation, *Advances in Atmospheric Sciences*, 26(4), 763–772, DOI: 10.1007/s00376-009-9029-z,  
 440 2009.
- Yuan, X., Wang, L., Wu, P., Ji, P., Sheffield, J., and Zhang, M.: Anthropogenic shift towards higher risk of flash drought over China, *Nature Communications*, 10, 4661, DOI: 10.1038/s41467-019-12692-7, 2019.
- Zhang, B., Kouchak, A.A., Yang, Y., Wei, J., and Wang, G.: A water-energy balance approach for multi-category drought assessment across globally diverse hydrological basins, *Agricultural and Forest Meteorology*, 264, 247–265, DOI:  
 445 10.1016/j.agrformet.2018.10.010, 2019a.
- Zhang, B., Xia, Y., Huning, L. S., Wei, J., Wang, G., and AghaKouchak, A.: A framework for global multicategory and multiscale drought characterization accounting for snow processes, *Water Resources Research*, 55, 9258–9278, DOI: 10.1029/2019WR025529, 2019b.
- Zhang, B., Zhao, X., Jin, J., and Wu, P.: Development and evaluation of a physically based multiscale drought index: The  
 450 Standardized Moisture Anomaly Index, *Journal of Geophysical Research: Atmospheres*, 120, 11575–11588, DOI: 10.1002/2015JD023772, 2015.
- Zhang, G., Su, X., Ayantobo, O.O., and Feng, K.: Drought monitoring and evaluation using ESA CCI and GLDAS-Noah soil moisture datasets across China, *Theoretical and Applied Climatology*, 144(3–4), 1407–1418, DOI: 10.1007/s00704-021-03609-w, 2021a.
- 455 Zhang, G., Su, X., Singh, V.P., and Ayantobo, O.O.: Appraising standardized moisture anomaly index (SZI) in drought projection across China under CMIP6 forcing scenarios, *Journal of Hydrology: Regional Studies*, 37, 100898, DOI: 10.1016/j.ejrh.2021.100898, 2021b.
- Zhang, Y., You, Q., Mao, G., Chen, C., and Ye, Z.: Short-term concurrent drought and heatwave frequency with 1.5 and 2.0 °C global warming in humid subtropical basins: A case study in the Gan River Basin, China, *Climate Dynamics*, 52(7–8),  
 460 4621–4641, DOI: 10.1007/s00382-018-4398-6, 2018.
- Zhou, S., Williams, A.P., Berg, A.M., Cook, B. I., Zhang, Y., Hagemann, S., ... and Gentile, P.: Land–atmosphere feedbacks exacerbate concurrent soil drought and atmospheric aridity, *Proceedings of the National Academy of Sciences*, 116(38), 18848–18853, DOI: 10.1073/pnas.1904955116, 2019.
- Zscheischler, J., Martius, O., Westra, S., Bevacqua, E., Raymond, C., Horton, R. M., ... and Vignotto, E.: A typology of  
 465 compound weather and climate events, *Nature Reviews Earth & Environment*, 1(7), 333–347, DOI: 10.1038/s43017-020-0060-z, 2020.



- Zscheischler, J., Michalak, A. M., Schwalm, C., Mahecha, M. D., Huntzinger, D. N., Reichstein, M., ... and Zeng, N.: Impact of large-scale climate extremes on biospheric carbon fluxes: An intercomparison based on MsTMIP data, *Global Biogeochemical Cycles*, 28(6), 585–600, DOI: 10.1002/2014gb004826, 2014.
- 470 Zscheischler, J., Westra, S., van den Hurk, B. J. J. M., Seneviratne, S. I., Ward, P. J., Pitman, A., ... and Zhang, X.: Future climate risk from compound events, *Nature Climate Change*, 8(6), 469–477, DOI: 10.1038/s41558-018-0156-3, 2018